Frontiers International Conference on Wastewater TreatMent

21-24 MAY 2017 | PALERMO – ITALY

Reaction extents: A divide-and-conquer approach for kinetic model identification

A. Masic*, J. Billeter**, D. Bonvin**, K. Villez*,
* Eawag: Swiss Federal Institute of Aquatic Science and Technology, Überlandstrasse 133, CH-8600 Dübendorf, Switzerland
** Laboratoire d'Automatique, Ecole Polytechnique Fédérale de Lausanne, CH-1015 Lausanne, Switzerland

Biological wastewater treatment; Extents; Model identification; Resource recovery; Parameter estimation; Urine nitrification

Introduction

Obtaining reliable wastewater treatment process models is critical for the application of model-based design, operation, and automation. For example, Masic *et al.* (2014) explored the use of an observer designed for nonlinear processes to estimate nitrite in a biological urine nitrification process. In this process, anthropogenic urine is used as a resource for the production of a fertilizer (Udert & Wächter, 2012). Thanks to the separated collection and treatment of urine via NoMix toilets (Larsen *et al.,* 2001), the majority of the nitrogen and phosphorus released via human excreta is captured. The urine nitrification step has two purposes: to prevent *(i)* volatilization of ammonia by reducing the pH and *(ii)* production of malodourous compounds. If successful, one can store nitrified urine for long periods of time.
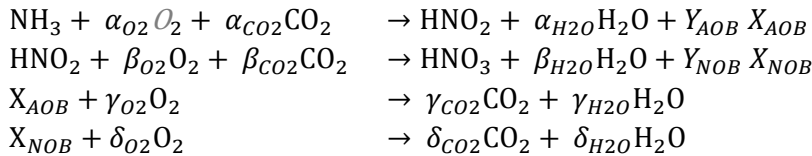
The urine nitrification process operates at fairly high conversion rates and is prone to three important failures. The first failure is caused by inhibition of the ammonia oxidizing bacteria (AOB) at high free ammonia concentrations and can lead to washout of AOB as well as the nitrite oxidizing bacteria (NOB). The second failure is caused by growth of acid-tolerant AOB and causes the pH to decrease to a level where the NOB are inhibited and undesired chemical reactions occur. The third failure appears when a temporary accumulation of nitrite causes NOB inhibition, thereby reducing their activity. Such a nitrite accumulation can lead to an irrecoverable failure if the nitrite is allowed to accumulate to high levels (above 50 mg N/L). The first and second failures are mitigated easily by maintaining a safe pH via manipulation of the urine feed flow rate. The third failure is more difficult to avoid and requires a timely detection of nitrite. Masic *et al.* (2014) provided successful preliminary tests with a model-based observer, which highly depends on the availability of a reliable model.

It is unlikely that standard parameter values apply due to the high-strength nature of human urine. For this reason, a well-calibrated model is desired. In Masic *et al.* (2016b) parameters were estimated to global optimality for the nitrite oxidation by NOB. The applied method, however, allows only estimating parameters of a single reaction system. To apply the same optimization method to multivariate processes, an extent-based methodology was tested in silico in Masic *et al.* (2016a). By means of the computation of reaction extents, one can separate the estimation of the parameters for each individual reaction. This extent-based modelling method however requires as many measured variables as the number of reactions (Rodrigues *et al.,* 2015). For this reason, Masic *et al.* (2016a) simplified the model identification problem by considering a constant biomass, i.e. a net biomass growth equal to zero for both AOB and NOB. In the present study, the extent-based model identification method is modified to avoid this simplification, while allowing the application of the globally optimal parameter estimation procedure developed in Masic *et al.* (2016b). At the same time, the resulting model identification method is tested with experimental data for the first time.

Methods

Model structure. The nitrification process is modeled according to the following reaction scheme involving two growth reactions and decay reactions:

$$
\begin{aligned}
NH_3 + \alpha_{O2} O_2 + \alpha_{CO2} CO_2 &\rightarrow HNO_2 + \alpha_{H2O} H_2O + Y_{AOB} X_{AOB} \\
HNO_2 + \beta_{O2} O_2 + \beta_{CO2} CO_2 &\rightarrow HNO_3 + \beta_{H2O} H_2O + Y_{NOB} X_{NOB} \\
X_{AOB} + \gamma_{O2} O_2 &\rightarrow \gamma_{CO2} CO_2 + \gamma_{H2O} H_2O \\
X_{NOB} + \delta_{O2} O_2 &\rightarrow \delta_{CO2} CO_2 + \delta_{H2O} H_2O
\end{aligned}
$$

with X_{AOB} and X_{NOB} the AOB and NOB biomasses, and Y_{AOB} and Y_{NOB} the yield coefficients. This reaction system has $S = 7$ species involved in $R = 4$ reactions. The internalization of nitrogen into the biomass is currently ignored. The complete model is written as:

$$\dot{\mathbf{c}}(t) = \mathbf{N}^T \mathbf{r}(\mathbf{c}(t), \boldsymbol{\theta}), \qquad \mathbf{y}_h = \mathbf{G}\, \mathbf{c}(t_h), \qquad \mathbf{c}(0) = \mathbf{c}_0 \qquad \text{Eq. 1}$$

$$\tilde{\mathbf{y}}_h = \mathbf{y}_h + \boldsymbol{\epsilon}_h \qquad\qquad \boldsymbol{\epsilon}_h \sim \mathcal{N}(\mathbf{0}, \boldsymbol{\Sigma}_h) \qquad\qquad\qquad \text{Eq. 2}$$

with $\mathbf{c}$ the S-dimensional concentration vector, $\mathbf{r}$ the R-dimensional vector of reaction rates, N the $R \times S$ stoichiometric matrix, $\tilde{\mathbf{y}}$ the M-dimensional measurement vector, $\mathbf{G}$ the $M \times S$ measurement matrix, where M denotes the number of measured quantities, ϵ the measurement error vector, $\boldsymbol{\Sigma}_h$ the measurement error variance-covariance matrix, and h the sampling index ($h = 1, 2, \dots, H$). In this work, the rate law expressions $\mathbf{r}(\mathbf{c}(t), \boldsymbol{\theta})$ and the initial conditions $\mathbf{c}_0$ are assumed to be known. One also assumes that the elements of $\boldsymbol{\theta}$ are either known or structurally identifiable (as in Dochain *et al.,* 1995 and Petersen *et al.,* 2003).

According to Eqs. 1-2, the following arrays apply to the nitrification process:

$$\mathbf{c} = [c_{TAN}\ c_{TNO_2}\ c_{TNO_3}\ c_{AOB}\ c_{NOB}]^T, \qquad \mathbf{G} = \begin{bmatrix} 1 & 0 & 0 & 0 & 0 \\ 0 & 1 & 0 & 0 & 0 \end{bmatrix} \qquad \text{Eq. 3}$$

$$\mathbf{N} = \begin{bmatrix} -1 & 1 & 0 & Y_{AOB} & 0 \\ 0 & -1 & 1 & 0 & Y_{NOB} \\ 0 & 0 & 0 & -1 & 0 \\ 0 & 0 & 0 & 0 & -1 \end{bmatrix}, \qquad \mathbf{r} = \begin{bmatrix} \mu_{AOB} c_{AOB} \frac{c_{TAN}}{K_{AOB} + c_{TAN}} \\ \mu_{NOB} c_{NOB} \frac{c_{TNO_2}}{K_{NOB} + c_{TNO_2}} \\ b_{AOB} c_{AOB} \\ b_{NOB} c_{NOB} \end{bmatrix} \qquad \text{Eq. 4}$$

where $\mathbf{c}$ contains the total ammonia, total nitrite, total nitrate, AOB, and NOB concentrations (in this order). The matrix $\mathbf{G}$ indicates that the concentrations of ammonia and nitrite are measured. The stoichiometric matrix N includes the unknown yield coefficients. The kinetic parameters are the maximum specific growth rates (μ_{AOB}, μ_{NOB}), the affinity constants (K_{AOB}, K_{NOB}), and the specific decay rates (b_{AOB}, b_{NOB}).

Extent computation. In the studied case, the structure of $\mathbf{G}$ and $\mathbf{N}$ allows computing the accumulated numbers of moles of ammonia converted through the AOB growth reaction and the accumulated numbers of moles of nitrite converted through the NOB growth reaction:

$$\mathbf{x}_h = \left(\mathbf{G}\, \mathbf{N}^T\, \mathbf{S}^T\right)^+ (\tilde{\mathbf{y}}_h - \mathbf{G}\, \mathbf{c}_0) \qquad\qquad \text{Eq. 5}$$

Eq. 5 defines the *experimental extents of the growth reactions*. In the above formula, $\mathbf{S}$ is a selection matrix that is used to select the growth reactions from all reactions:

$$\mathbf{S} = \begin{bmatrix} 1 & 0 & 0 & 0 \\ 0 & 1 & 0 & 0 \end{bmatrix} \qquad\qquad \text{Eq. 6}$$

Parameter estimation. Once the experimental extents of the growth reactions are available, one can start the parameter estimation. This estimation is executed separately for each

bacterial group. This means that estimates for μ_{AOB}, K_{AOB}, b_{AOB}, and Y_{AOB} and estimates for μ_{NOB}, K_{NOB}, b_{NOB}, and Y_{NOB} are obtained by solving two distinct optimization problems. For the AOB-related parameters, one simulates the growth and decay of the AOB and finds those parameters that minimize the sum of squared residuals between the simulated and experimental extent of the AOB growth reaction. Note that simulating the growth and decay of the AOB does not require any information regarding the NOB-related processes. A similar approach is used for NOB-related parameters. In this case, the progress of the AOB growth influences the nitrite concentration that appears in the NOB growth rate expression. To account for this, the nitrite produced through AOB growth is expressed equivalently as the extent of the AOB growth reaction. To avoid simulation of the AOB-related processes during NOB-related parameter estimation, the experimental extent for the AOB growth is interpolated and used as a proxy for the produced amounts of nitrite.

Results

The ammonia and nitrite concentration measurements obtained in a single cycle of the intermittently fed urine nitrification process are shown in Figure 1. One can see that the ammonia concentration decays monotonically. The nitrite concentration reaches its maximum around 6 hours after feeding.

Figures 2 displays the extents obtained via Eqs. 5-6, namely, the volume-specific extent of the AOB growth reaction (first extent), and the volume-specific extent of the NOB growth reaction (second extent). The first extent (AOB growth) is modelled by simulating the AOB growth and decay reactions while adjusting the parameters μ_{AOB}, K_{AOB}, b_{AOB}, and Y_{AOB}. The extent simulated with the optimal parameter estimates is shown in the left panel of Figure 2. The same procedure is applied to the second extent. The experimental extent of the AOB growth reaction are interpolated to enable the simulation of the produced nitrite. The simulated extent of the NOB growth reaction after estimation of μ_{NOB}, K_{NOB}, b_{NOB}, and Y_{NOB} is shown in the right panel of Figure 2. The simulated and experimental extents are in good agreement.

The resulting fitted parameters are then used to simulate the complete model (Eqs. 1-4). The simulated ammonia and nitrite concentrations are shown in Figure 1. The obtained model fits the concentration data very well, despite the separated estimation of the parameters.

Conclusions

This contribution shows that simultaneous estimation of all kinetic parameters in a biokinetic wastewater treatment process model is not necessary. Instead, the computation of extents allows separating the parameter estimation problem into multiple smaller problems, each one involving only the estimation of a fraction of the parameters. This was demonstrated with an experimental data set collected in an intermittently fed urine nitrification process for recovery of nitrogen and phosphorus in the form of a liquid fertilizer.

References

Dochain D, Vanrolleghem P A, Van Daele M (1995). Structural identifiability of biokinetic models of activated sludge respiration. *Wat. Res.,* **29**, 2571-2578.
Larsen T A, Peters I, Alder A, Eggen R, Maurer M, Muncke J (2001). Peer reviewed: re-engineering the toilet for sustainable wastewater management. *Env. Sci. Technol.*, **35,** 192A-197A.
Masic A, Villez K (2014). Model-based observers for monitoring of a biological nitrification process for decentralized wastewater treatment – Initial results. *2nd IWA Specialized International Conference Ecotechnologies for Wastewater Treatment (EcoSTP2014)*, Verona, Italy, June 23–25, 2014, 402–405.

Masic A, Srinivasan S, Billeter J, Bonvin D, Villez K (2016a). Biokinetic model identification via extents of reaction. *5th IWA/WEF Wastewater Treatment Modelling Seminar (WWTmod2016),* Annecy, France, April 2-6, 2016, appeared on USB-stick.

Masic A, Udert K, Villez K (2016b). Global parameter optimization for biokinetic modeling of simple batch experiments. *Environ. Modell. and Softw.,* **85,** 356-373.

Petersen B, Gernaey K, Devisscher M, Dochain D, Vanrolleghem P A (2003). A simplified method to assess structurally identifiable parameters in Monod-based activated sludge models. *Wat. Res.,* **37**, 2893-2904.

Rodrigues D, Srinivasan S, Billeter J, Bonvin D (2015). Variant and invariant states for chemical reaction systems. *Comp. Chem. Eng.,* **73,** 23-33.

Udert K M, Wächter M (2012). Complete nutrient recovery from source-separated urine by nitrification and distillation. *Wat. Res.,* **46,** 453-464.
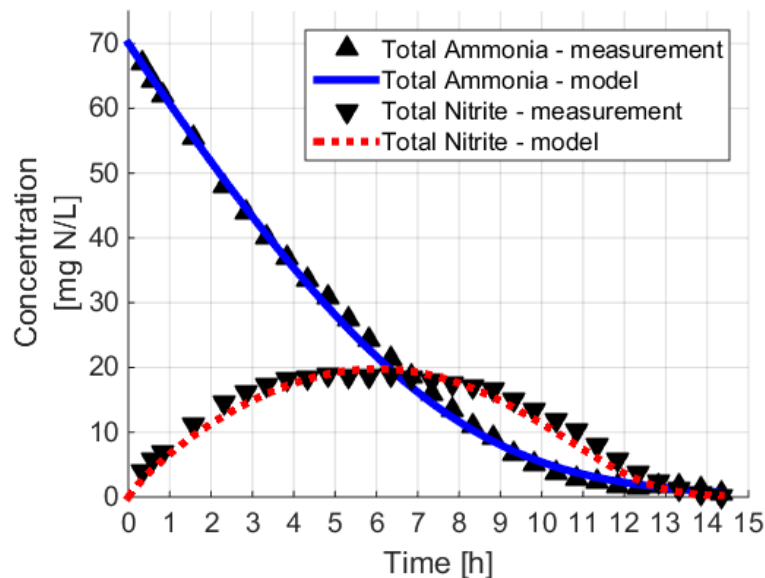
Figure 1. *Experimental (triangles) and fitted (lines) concentrations are in good agreement.*
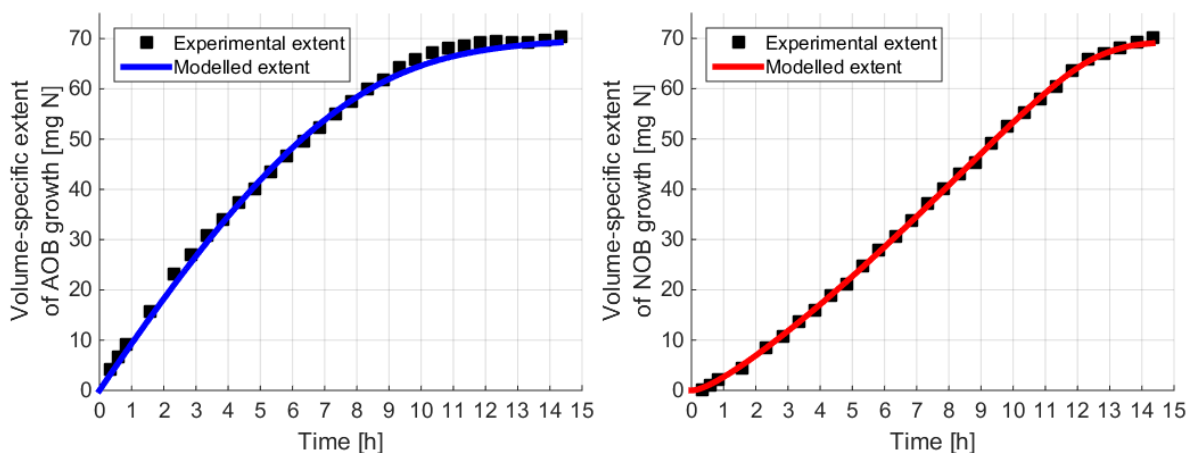

Figure 2. *Experimental (squares) and simulated (lines) extents of the AOB growth reaction (left) and of the NOB growth reaction (right).*